

# Mechanisms controlling the sensitivity of amperometric biosensors in flow injection analysis systems

Darius Baronas · Feliksas Ivanauskas ·  
Romas Baronas

Received: 8 January 2011 / Accepted: 4 May 2011 / Published online: 15 May 2011  
© Springer Science+Business Media, LLC 2011

**Abstract** This paper numerically investigates the sensitivity of an amperometric biosensor acting in the flow injection mode when the biosensor contacts an analyte for a short time. The analytical system is modelled by non-stationary reaction-diffusion equations containing a non-linear term related to the Michaelis-Menten kinetics of an enzymatic reaction. The mathematical model involves three regions: the enzyme layer where enzymatic reaction as well as the mass transport by diffusion takes place, a diffusion limiting region where only the diffusion takes place, and a convective region. The biosensor operation is analysed with a special emphasis to the conditions at which the biosensor sensitivity can be increased and the calibration curve can be prolonged by changing the injection duration, the permeability of the external diffusion layer, the thickness of the enzyme layer and the catalytic activity of the enzyme. The apparent Michaelis constant is used as a main characteristic of the sensitivity and the calibration curve of the biosensor. The numerical simulation was carried out using the finite difference technique.

**Keywords** Modelling · Reaction-diffusion · Biosensor · Flow injection analysis

## 1 Introduction

Biosensors are analytical devices combined of biologically active substance, usually an enzyme, and a physicochemical transducer converting biochemical reaction result

---

D. Baronas (✉)

Institute of Mathematics and Informatics, Vilnius University, Akademijos 4, 08663 Vilnius, Lithuania  
e-mail: darius.baronas@mif.vu.lt

F. Ivanauskas · R. Baronas

Faculty of Mathematics and Informatics, Vilnius University, Naugarduko 24, 03225 Vilnius, Lithuania

to measurable quantity [1–3]. Biosensors are classified by their transducer extraction. Amperometric biosensors measure the current change on the working electrode due to the direct oxidation or reduction of chemical reaction products. The measured current is usually proportional to the concentration of the analyte (substrate). The amperometric biosensors are relatively cheap, sensitive and reliable devices for clinical diagnostics, drug detection, food analysis and environment monitoring [4–7].

The biosensors are combined with flow injection analysis (FIA) for on-line monitoring of raw materials, product quality and the manufacturing process [8–10]. In the FIA a biosensor contacts with the substrate for short time (seconds to tens of seconds) whereas in the batch analysis the biosensor remains immersed in the substrate solution for a long time [11]. Compared to the batch systems, the FIA systems present the advantages of the reduction in analysis time allowing a high sample throughput, and the possibility to work with small volumes of the substrate [12–14]. The FIA arrangement also presents a wide response range and high sensitivity [15, 16].

When designing biosensors the understanding their kinetic peculiarities is of crucial importance. To improve the efficiency of the development of a novel biosensor and to optimize its configuration the biosensor should be modelled [17–19]. Starting from the seventies various mathematical models have been successfully used as important tools to study and optimize analytical characteristics of actual biosensors [20–22]. A comprehensive review on the modelling of the amperometric biosensors has been presented by Schulmeister [23] and more recently by Baronas et al. [24].

Actual biosensors acting in the FIA mode have been already modelled usually at internal diffusion limitations by ignoring the external diffusion [25, 26]. However, in practical biosensing systems, the mass transport outside the enzyme region is of crucial importance, and it has to be taken into consideration when modelling the biosensor action [19, 27, 28]. Theoretical investigation of the FIA biosensing systems presented a higher quality of the concentrations prediction than the corresponding batch systems [26, 29].

This paper presents results of the biosensor modelling at mixed the enzyme kinetics, the external and internal diffusion limitations in the FIA. The biosensing system is modelled by non-stationary reaction-diffusion equations containing a non-linear term related to the Michaelis-Menten kinetics of an enzymatic reaction [24, 30]. The biosensor operation is analysed with a special emphasis to the conditions at which the biosensor sensitivity can be increased and the calibration curve can be prolonged by changing the injection duration, the permeability of the external diffusion layer, the thickness of the enzyme layer and the catalytic activity of the enzyme. The apparent Michaelis constant is used as one of the main characteristics of the sensitivity and the calibration curve of the biosensor [1, 3, 28, 31, 32]. The numerical simulation was carried out using the finite difference technique [24, 30].

## 2 Mathematical model

The amperometric biosensor is considered as an electrode and a relatively thin layer of an enzyme (enzyme membrane) applied onto the electrode surface. The biosensor model involves three regions: the enzyme layer (membrane) where the enzymatic

reaction as well as the mass transport by diffusion takes place, a diffusion limiting region where only the diffusion takes place, and a convective region.

In the enzyme layer we consider the enzyme-catalyzed reaction



where the substrate (S) combines reversibly with an enzyme (E) to form a complex (ES). The complex then dissociates into the product (P) and the enzyme is regenerated [1,3].

Assuming the quasi steady-state approximation, the concentration of the intermediate complex (ES) does not change and may be neglected when modelling the biochemical behaviour of biosensors [2,3,33]. In the resulting scheme, the substrate (S) is enzymatically converted to the product (P),



### 2.1 Governing equations

Assuming the symmetrical geometry of the electrode and a homogeneous distribution of the immobilized enzyme in the enzyme layer of a uniform thickness, the mathematical model of the biosensor action can be defined in a one-dimensional-in-space domain [23,24,34]. Coupling the enzyme catalyzed reaction (2) in the enzyme layer with the mass transport by diffusion, described by Fick’s law, leads to the following system of the reaction diffusion equations:

$$\frac{\partial S_1}{\partial t} = D_{S_1} \frac{\partial^2 S_1}{\partial x^2} - \frac{V_{\max} S_1}{K_M + S_1}, \tag{3a}$$

$$\frac{\partial P_1}{\partial t} = D_{P_1} \frac{\partial^2 P_1}{\partial x^2} + \frac{V_{\max} S_1}{K_M + S_1}, \quad x \in (0, d), \quad t > 0, \tag{3b}$$

where  $x$  and  $t$  stand for space and time,  $S_1$  and  $P_1$  are the concentrations of the substrate (S) and the product (P) in the enzyme layer,  $D_{S_1}$ ,  $D_{P_1}$  are the diffusion coefficients,  $V_{\max}$  is the maximal enzymatic rate attainable with that amount of the enzyme, when the enzyme is fully saturated with the substrate,  $K_M$  is the Michaelis constant, and  $d$  is the thickness of the enzyme layer [21–23]. The Michaelis constant  $K_M$  is the concentration of the substrate at which the reaction rate is half its maximum value  $V_{\max}$ .

In the outer layer only the mass transport by diffusion of both species takes place. We assume that the outer mass transport obeys a finite diffusion regime,

$$\frac{\partial S_2}{\partial t} = D_{S_2} \frac{\partial^2 S_2}{\partial x^2}, \tag{4a}$$

$$\frac{\partial P_2}{\partial t} = D_{P_2} \frac{\partial^2 P_2}{\partial x^2}, \quad x \in (d, d + \delta), \quad t > 0, \tag{4b}$$

where  $S_2$  and  $P_2$  are the substrate and the product concentrations in the outer layer,  $D_{S_2}$  and  $D_{P_2}$  are the diffusion coefficients, and  $\delta$  is the thickness of the diffusion layer.

## 2.2 Initial and boundary conditions

Let  $x = 0$  represent the surface of the electrode, while  $x = d + \delta$  is the farther boundary of the diffusion layer. The biosensor operation starts when the substrate appears in the bulk solution ( $t = 0$ ),

$$P_1(x, 0) = 0, \quad S_1(x, 0) = 0, \quad x \in [0, d], \quad (5a)$$

$$P_2(x, 0) = 0, \quad x \in [d, d + \delta], \quad (5b)$$

$$S_2(x, 0) = \begin{cases} 0, & x \in [d, d + \delta), \\ S_0, & x = d + \delta, \end{cases} \quad (5c)$$

where  $S_0$  is the substrate concentration in the bulk solution.

During the biosensor operation, the substrate penetrates through diffusion layer and reaches farther boundary of the enzyme layer ( $x = d$ ), where we define the matching conditions ( $t > 0$ ):

$$D_{S_1} \frac{\partial S_1}{\partial x} \Big|_{x=d} = D_{S_2} \frac{\partial S_2}{\partial x} \Big|_{x=d}, \quad S_1(d, t) = S_2(d, t), \quad (6a)$$

$$D_{P_1} \frac{\partial P_1}{\partial x} \Big|_{x=d} = D_{P_2} \frac{\partial P_2}{\partial x} \Big|_{x=d}, \quad P_1(d, t) = P_2(d, t). \quad (6b)$$

It is shown by these conditions that amount of the substrate which penetrated through the diffusion layer enters to the enzyme membrane.

Due to the electrode polarization the concentration of the reaction product at the electrode surface is permanently reduced to zero [23, 24]. The substrate concentration flux on the electrode surface equals zero because of the substrate electro-inactivity,

$$P_1(0, t) = 0, \quad \frac{\partial S_1}{\partial x} \Big|_{x=0} = 0. \quad (7)$$

The outer diffusion layer ( $d < x < d + \delta$ ) is treated as the Nernst diffusion layer [30]. According to the Nernst approach the layer of the thickness  $\delta$  remains unchanged with time, and away from it the solution is uniform in the concentration ( $t > 0$ ). In the FIA mode of the biosensor operation, the substrate appears in the bulk solution only for a short time period called the injection time. Later, the substrate disappears from the bulk solution,

$$P_2(d + \delta, t) = 0, \quad S_2(d + \delta, t) = \begin{cases} S_0, & t \leq T_F, \\ 0, & t > T_F, \end{cases} \quad (8)$$

where  $T_F$  is the injection time.

### 2.3 Biosensor response

The anodic or cathodic current is measured as a result of a physical experiment. The current is proportional to the gradient of the reaction product concentration at the electrode surface, i.e. on the border  $x = 0$ . The density  $I(t)$  of the biosensor current at time  $t$  can be obtained explicitly from Faraday's and Fick's laws [23],

$$I(t) = n_e F D_{P_1} \left. \frac{\partial P_1}{\partial x} \right|_{x=0}, \quad (9)$$

where  $n_e$  is a number of electrons involved in a charge transfer, and  $F$  is the Faraday constant.

We assume that the system reaches equilibrium when  $t \rightarrow \infty$ . The steady-state current is the main characteristic in commercial amperometric biosensors acting in the batch mode [1–3]. In the FIA, due to the zero concentration of the surrounding substrate at  $t > T_F$ , the steady-state current falls to zero,  $I(t) \rightarrow 0$ , when  $t \rightarrow \infty$ . Because of this, the steady-state current is not practically useful in the FIA systems. Since the current density  $I(t)$  of the biosensor acting in the injection mode is a non-monotonous function, the maximal current is one of the mostly used characteristics for this kind of the biosensors,

$$I_{\max} = \max_{t>0} \{I(t)\}, \quad (10)$$

where  $I_{\max}$  is the maximal density of the biosensor current.

### 2.4 Apparent Michaelis constant

In the Michaelis-Menten kinetic model, the Michaelis constant  $K_M$  is an approximation of the enzyme affinity for the substrate based on the rate constants within the reactions (1),  $K_M = (k_{-1} + k_2)/k_1$ , and it is numerically equivalent to the substrate concentration at which half the maximum rate of the enzyme-catalyzed reaction is achieved [1, 3].

Under certain conditions, especially under diffusional limitations for the substrate, the apparent Michaelis constant  $K_{M,app}$  can differ from  $K_M$  for the same catalytic process. This known phenomenon has been subjected to the theoretical modelling, and it has been shown that, under certain conditions, the apparent Michaelis constant highly depends on the biosensor geometry [28]. Also, a substantial increase of the Michaelis constant has been shown at restricted diffusion of the substrate through an outer membrane covering an enzyme layer [32]. This result appears to be of a high practical interest, since it enables to expand the linear dependence of biosensor response on the substrate concentration towards the higher concentrations under the deep diffusion mode of the biosensor operation, whereas the response time increases not very drastic [32]. This property is especially attractive for biosensors acting in FIA mode because of a relatively short their response time [14, 26].

In this research, the apparent Michaelis constant  $K_{M,app}$  was accepted as a main characteristic of the sensitivity and of the calibration curve of the amperometric biosensors [1,3,32]. The greater value of  $K_{M,app}$  corresponds to a wider range of the linear part of the calibration curve. In the case of the batch analysis, the  $K_{M,app}$  is usually defined with respect to the steady-state response. In the FIA, since the biosensor current steadies at zero, the constant  $K_{M,app}$  is defined with respect to the maximal current as the substrate concentration at a half-maximum biosensor activity,

$$K_{M,app} = \left\{ S_0^* : I_{\max}(S_0^*) = 0.5 \lim_{S_0 \rightarrow \infty} I_{\max}(S_0) \right\}, \quad (11)$$

where  $I_{\max}(S_0)$  is the maximal density of the biosensor current calculated at the substrate concentration  $S_0$ .

## 2.5 Dimensionless model

In order to extract the main governing parameters of the mathematical model, thus reducing a number of model parameters in general, a dimensionless model is often derived [17,23,35]. For simplicity, we introduce the concentrations  $S$  and  $P$  of the substrate and the product for the entire domain  $x \in [0, d + \delta](t \geq 0)$ ,

$$S = \begin{cases} S_1, & 0 \leq x \leq d, \\ S_2, & d < x \leq d + \delta, \end{cases} \quad (12a)$$

$$P = \begin{cases} P_1, & 0 \leq x \leq d, \\ P_2, & d < x \leq d + \delta. \end{cases} \quad (12b)$$

Both concentration functions ( $S$  and  $P$ ) are continuous in the entire domain  $x \in [0, d + \delta]$ . The replacement of the parameters is based on parameter mappings defined in Table (1).

**Table 1** Dimensional and dimensionless model parameters

Parameter	Dimensional	Dimensionless
Distance form electrode	$x$ , cm	$\hat{X} = x/d$
Time	$t$ , s	$\hat{T} = tD_{S_1}/d^2$
Injection time	$T_F$ , s	$\hat{T}_F = T_F D_{S_1}/d^2$
Enzyme layer thickness	$d$ , cm	$\hat{X} = d/d = 1$
Diffusion layer thickness	$\delta$ , cm	$\hat{\Delta} = \delta/d$
Substrate concentration	$S, S_0, M$	$\hat{S} = S/K_M, \hat{S}_0 = S_0/K_M$
Product concentration	$P, M$	$\hat{P} = P/K_M$
Michelis-Menten constant	$K_M, K_{M,app}, M$	$\hat{K}_M = K_M/K_M = 1, \hat{K}_{M,app} = K_{M,app}/K_M$
Current density	$I, I_{\max}$ , A cm <sup>-2</sup>	$\hat{I} = Id/(n_e F D_{P_1} K_M), \hat{I}_{\max} = I_{\max}d/(n_e F D_{P_1} K_M)$

For the enzyme layer, the reaction-diffusion Eqs. (3) can be rewritten as follows:

$$\frac{\partial \hat{S}}{\partial \hat{T}} = \frac{\partial^2 \hat{S}}{\partial \hat{X}^2} - \alpha^2 \frac{\hat{S}}{1 + \hat{S}}, \tag{13a}$$

$$\frac{\partial \hat{P}}{\partial \hat{T}} = \frac{D_{P_1}}{D_{S_1}} \frac{\partial^2 \hat{P}}{\partial \hat{X}^2} + \alpha^2 \frac{\hat{S}}{1 + \hat{S}}, \quad \hat{X} \in (0, 1), \quad \hat{T} > 0, \tag{13b}$$

where  $\alpha^2$  is the diffusion module, also known as Damköhler number [23],

$$\alpha^2 = \frac{d^2 V_{\max}}{D_{S_1} K_M}. \tag{14}$$

The diffusion module  $\alpha^2$  compares the rate of the enzyme reaction ( $V_{\max}/K_M$ ) with the rate of the mass transport through the enzyme layer ( $D_{S_1}/d^2$ ).

The diffusion Eqs. (4) are transformed as follows:

$$\frac{\partial \hat{S}}{\partial \hat{T}} = \frac{D_{S_2}}{D_{S_1}} \frac{\partial^2 \hat{S}}{\partial \hat{X}^2}, \tag{15a}$$

$$\frac{\partial \hat{P}}{\partial \hat{T}} = \frac{D_{P_2}}{D_{S_1}} \frac{\partial^2 \hat{P}}{\partial \hat{X}^2}, \quad \hat{X} \in (1, 1 + \hat{\Delta}), \quad \hat{T} > 0. \tag{15b}$$

The initial conditions (5) take the following form:

$$\hat{P}(\hat{X}, 0) = 0, \quad \hat{S}(\hat{X}, 0) = 0, \quad \hat{X} \in [0, 1 + \hat{\Delta}), \tag{16a}$$

$$\hat{P}(1 + \hat{\Delta}, 0) = 0, \quad \hat{S}(1 + \hat{\Delta}, 0) = \hat{S}_0. \tag{16b}$$

The matching conditions (6) transform to the following conditions ( $\hat{T} > 0$ ):

$$\left. \frac{\partial \hat{S}}{\partial \hat{X}} \right|_{\hat{X}=1} = \left. \frac{D_{S_2}}{D_{S_1}} \frac{\partial \hat{S}}{\partial \hat{X}} \right|_{\hat{X}=1}, \tag{17a}$$

$$\left. \frac{D_{P_1}}{D_{S_1}} \frac{\partial \hat{P}}{\partial \hat{X}} \right|_{\hat{X}=1} = \left. \frac{D_{P_2}}{D_{S_1}} \frac{\partial \hat{P}}{\partial \hat{X}} \right|_{\hat{X}=1}. \tag{17b}$$

The boundary conditions (7) and (8) take the following form ( $\hat{T} > 0$ ):

$$\hat{P}(0, \hat{T}) = 0, \quad \left. \frac{\partial \hat{S}}{\partial \hat{X}} \right|_{\hat{X}=0} = 0, \tag{18a}$$

$$\hat{P}(1 + \hat{\Delta}, \hat{T}) = 0, \quad \hat{S}(1 + \hat{\Delta}, \hat{T}) = \begin{cases} \hat{S}_0, & \hat{T} \leq \hat{T}_F, \\ 0, & \hat{T} > \hat{T}_F. \end{cases} \tag{18b}$$

The dimensionless current (flux)  $\hat{I}$  is defined as follows:

$$\hat{I}(\hat{T}) = \frac{\partial \hat{P}}{\partial \hat{X}} \Big|_{\hat{X}=0} = \frac{I(t)d}{n_e F D_{P_1} K_M}. \quad (19)$$

Assuming the same diffusion coefficients of both considering species, the substrate and the product, the initial collection of the model parameters reduces to a few aggregate parameters:  $\hat{\Delta}$  - the diffusion layer thickness,  $\alpha^2$  - the diffusion module,  $\hat{T}_F$  - the injection time,  $\hat{S}_0$  - the substrate concentration in the bulk during the injection, and  $\hat{D}_{21} = D_{S_2}/D_{S_1} = D_{P_2}/D_{P_1}$  - the dimensionless ratio of the diffusion coefficient in the diffusion layer to the corresponding diffusion coefficient in the enzyme layer. The diffusion module  $\alpha^2$  is one of the most important parameters essentially defining internal characteristics of an amperometric biosensor [21–24]. The biosensor response is known to be under diffusion control when  $\alpha^2 \gg 1$ . In the very opposite case, when  $\alpha^2 \ll 1$ , the enzyme kinetics predominates in the response.

The Biot number  $Bi$  is another dimensionless parameter widely used to indicate the internal mass transfer resistance to the external one [24, 35],

$$Bi = \frac{d/D_{S_1}}{\delta/D_{S_2}} = \frac{D_{S_2}d}{D_{S_1}\delta} = \hat{D}_{21} \frac{d}{\delta}. \quad (20)$$

### 3 Numerical simulation

No analytical solution is possible because of the nonlinearity of the governing equations of the mathematical model (3)–(9) [23, 34]. For this reason a numerical solution was performed. Solving the biosensor model, an implicit finite difference scheme was built on a uniform discrete grid [23, 24, 30, 36]. The computational model was developed in the C language [37].

The mathematical model and the numerical solution were validated using a known analytical solution [23]. Assuming  $T_F \rightarrow \infty$ , the mathematical model (3)–(9) approaches the two compartment model of the amperometric biosensor acting in the batch mode [23]. Additionally assuming  $S_0 \ll K_M$ , the nonlinear reaction (Michaelis-Menten) function in (3) simplifies to a linear function  $V_{\max} S_1/K_M$ . At these assumptions the model (3)–(9) has been analytically solved at the steady-state conditions [23].

A number of experiments were carried out, while values of some parameters were kept constant [38],

$$\begin{aligned} D_{S_1} = D_{P_1} = 300 \mu\text{m}^2/\text{s}, \quad D_{S_2} = 2D_{S_1}, \quad D_{P_2} = 2D_{P_1}, \\ K_M = 100 \mu\text{M}, \quad n_e = 1, \quad d = 200 \mu\text{m}. \end{aligned} \quad \begin{matrix} (21) \\ (22) \end{matrix}$$

Figure 1 shows the evolution of the density  $I(t)$  of the biosensor current. The biosensor action was simulated at a moderate concentration  $S_0$  of the substrate ( $S_0 = K_M$ ) and different values of the other model parameters, the dimensionless diffusion module  $\alpha^2$  (1 and 2), the injection time  $T_F$  (3 and 6 s) and the dimensionless Biot number



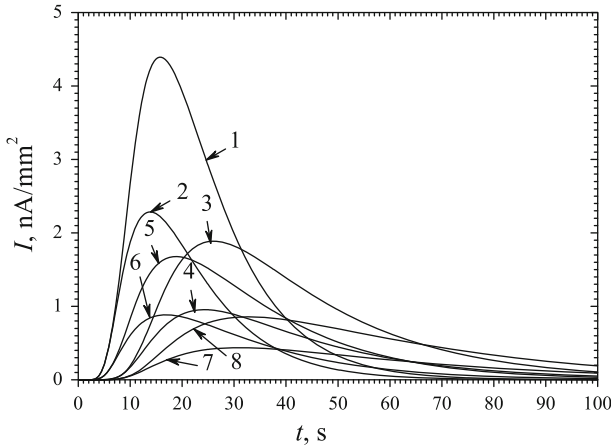


**Fig. 1** The dynamics of the biosensor response at different values of the diffusion module  $\alpha^2$ : 1 (5–8), 2 (1–4), the Biot number  $Bi$ : 1 (3, 4, 7, 8), 2 (1, 2, 5, 6) and the injection time  $T_F$ : 3 (2, 4, 6, 8), 6 s (1, 3, 5, 7)

$Bi$  (1 and 2). Assuming (22), these two values (1 and 2) of  $\alpha^2$  were obtained at the following values of the maximal enzymatic rate  $V_{max}$ : 0.75 and 1.5  $\mu\text{M}$ , respectively. Accordingly,  $Bi = 2$  corresponds to the thickness  $\delta$  of the external diffusion layer equal to the thickness  $d$  of the enzyme layer, while  $Bi = 1$  at  $\delta = \hat{D}_{21}d = 2d = 400 \mu\text{m}$ .

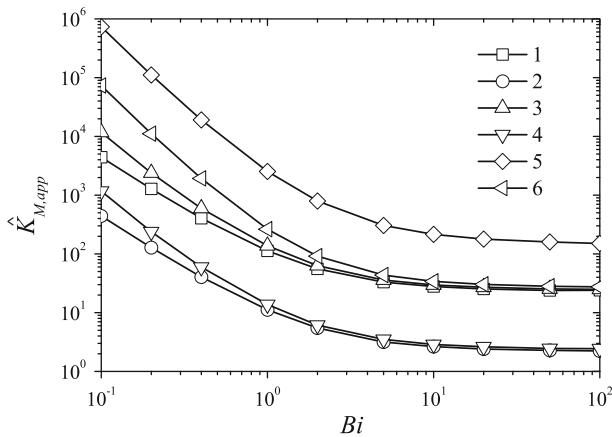
One can see in Fig. 1 the non-monotonic behavior of the biosensor current. In all the cases the current increases during the injection period ( $t \leq T_F$ ). However, the current also increases some time after the substrate disappearing from the bulk solution ( $t \geq T_F$ ). The time moment of the maximum current as well as the maximal current itself depend on all three model parameters:  $\alpha^2$ ,  $Bi$  and  $T_F$ .

Figure 1 shows that the density  $I_{max}$  of the maximal current increases almost 2 times when the injection time  $T_F$  doubles. However, the influence of the doubling the time  $T_F$  on the time of the maximal current is rather slight. When comparing curves 1 ( $T_F = 6$ ) and 2 ( $T_F = 3$  s) one can see that the time of the maximal response increases from 13.9 only to 16 s, while  $I_{max}$  increases from 2.3 event to 4.4 nA/mm<sup>2</sup> at  $\alpha^2 = 2$ ,  $Bi = 2$ .

Figure 1 also shows that the biosensor response significantly depends on the Biot number  $Bi$ . A decrease in  $Bi$  noticeable prolongs the response. As one can see in Fig. 1 that the maximal current decreases when the thickness of the external diffusion layer increases, i.e.  $Bi$  decreases. FIA biosensing systems have been already investigated by using mathematical models at zero thickness ( $Bi \rightarrow \infty$ ) of the external diffusion layer [26,29]. Figure 1 visually substantiates the importance of the external diffusion layer.

#### 4 Results and discussion

Using the numerical simulation, the biosensor operation was analysed with a special emphasis to the conditions at which the biosensor sensitivity can be increased and the calibration curve can be prolonged by changing the injection duration, the biosensor



**Fig. 2** The dependence of the apparent Michaelis constant  $\hat{K}_{M,app}$  on the Biot number  $Bi$  at different values of the diffusion module  $\alpha^2$ : 0.1 (1, 2), 1 (3, 4), 10 (5, 6) and the injection time  $T_F$ : 1 (1, 3, 5), 10 s (2, 4, 6)

geometry and the catalytic activity of the enzyme. In order to investigate the influence of the model parameters on the apparent Michaelis constant  $\hat{K}_{M,app}$ , the simulation was performed at wide ranges of the values of the diffusion module  $\alpha^2$ , the Biot number  $Bi$  and the injection time  $T_F$ . Since in the FIA, the injection usually continues several seconds (neither minutes nor milliseconds), to render the injection time more lucidly we used the dimensional injection time  $T_F$  instead of the dimensionless injection time  $\hat{T}_F$ .

The constant  $\hat{K}_{M,app}$  expresses the relative prolongation (in times) of the calibration curve in comparison with the theoretical Michaelis constant  $K_M$ . For the biosensor of a concrete configuration, the  $\hat{K}_{M,app}$  can be rather easily calculated by multiple simulation of the maximal response changing the substrate concentration  $\hat{S}_0$ .

Figure 2 shows the dependence of the apparent Michaelis constant  $\hat{K}_{M,app}$  on the Biot number  $Bi$ . The constant  $\hat{K}_{M,app}$  was calculated at three values of the diffusion module  $\alpha^2$ : 0.1 (curves 1 and 2), 1 (3, 4) and 10 (5, 6), and two practically extreme values of the injection time  $T_F$ : 1 (1, 3, 5) and 10 s (2, 4, 6). At concrete values of  $\alpha^2$  and  $T_F$ , the calculations were performed by changing the thickness  $\delta$  of the diffusion layer from  $40 \mu\text{m}$  ( $\delta = 0.2d$ ) to  $4 \text{ mm}$  ( $\delta = 20d$ ) and keeping constant the thickness  $d = 200 \mu\text{m}$  of the enzyme layer.

One can see in Fig. 2, that at relatively large values of the Biot number ( $Bi > 10$ ) the apparent Michaelis constant  $\hat{K}_{M,app}$  (as well as dimensional  $K_{M,app}$ ) is almost insensitive to changes in  $Bi$ . However, when  $Bi < 1$  a decrease in  $Bi$  affects a drastic increase of  $\hat{K}_{M,app}$ . By increasing the thickness  $\delta$  of the external diffusion layer as well as decreasing the diffusivity  $D_{S_2}$  in this layer, i.e. by decreasing  $Bi$ , the calibration curve of the biosensor can be prolonged by a few orders of magnitude. The diffusivity of species in diffusion layer is usually relative to the permeability of the diffusion layer. The Biot number  $Bi$  might be also decreased by decreasing the permeability of the external diffusion layer.

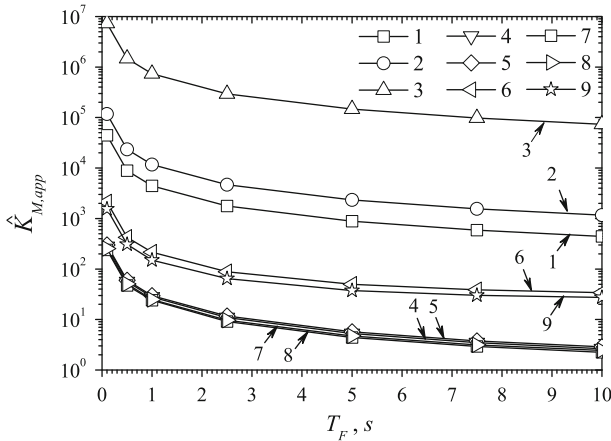


**Fig. 3** The apparent Michaelis constant  $\hat{K}_{M,app}$  versus the injection time  $T_F$ ,  $\alpha^2$ : 0.1 (1, 4, 7), 1 (2, 5, 8), 10 (3, 6, 9),  $Bi$ : 0.1 (1–3), 10 (4–6), 100 (7–9)

In the case of the batch analysis, an advantageous effect of the external diffusivity on the length of the calibration curve of amperometric biosensors is rather well known [1,3,28,32]. Figure 2 shows that, due to the FIA, the linear part of the calibration curve becomes even longer. This figure also shows a weak dependence of  $\hat{K}_{M,app}$  on the diffusion module  $\alpha^2$  when  $\alpha^2 \leq 1$ .

To properly investigate the impact of the injection time  $T_F$  on the length of the linear part of the calibration curve, the apparent Michaelis constant  $\hat{K}_{M,app}$  was calculated by changing  $T_F$  from 1 up to 10 s. Values of  $\hat{K}_{M,app}$  were calculated at three values of the diffusion module  $\alpha^2$  (0.1, 1 and 10) and three values of the Biot number  $Bi$  (0.1, 10 and 100). The calculation results are depicted in Fig. 3.

As one can see in Fig. 3 that  $\hat{K}_{M,app}$  exponentially increases with a decrease in the injection time  $T_F$ . The calibration curve of the biosensor can be prolonged by a few orders of magnitude only by decreasing the injection time  $T_F$ . The impact of  $T_F$  is practically invariant to the Biot number  $Bi$  and the diffusion module  $\alpha^2$ . The exponential increase is specifically characteristic at low values of  $T_F$  ( $T_F < 3$  s).

One can also see in Fig. 3 no noticeable difference between curves 4, 5, 7 and 8. Two other curves 6 and 9 only slightly differs from each other. So, at relatively high values of the Biot number ( $Bi \geq 10$ ), the  $\hat{K}_{M,app}$  is only slightly sensitive to changes in  $Bi$ . This effect was even more easily shown in Fig. 2. Figure 3 additionally shows that the  $\hat{K}_{M,app}$  more increases at greater values of the diffusion module  $\alpha^2$  rather than at lower ones.

Finally, the impact of the diffusion module  $\alpha^2$  on the apparent Michaelis constant was evaluated. The result is presented in Fig. 4. The constant  $\hat{K}_{M,app}$  was calculated at three values of the diffusion Biot number  $Bi$ : 0.1 (curves 1 and 4), 10 (2, 5) and 100 (3, 6), and two values of the injection time  $T_F$ : 1 (1–3) and 10 s (4–6). At concrete values of  $Bi$  and  $T_F$ , the calculations were performed by changing the maximal enzymatic rate  $V_{max}$  from 75 nM/s ( $\alpha^2 = 0.1$ ) to 7.5  $\mu$ M/s ( $\alpha^2 = 10$ ) and keeping other parameters constant.

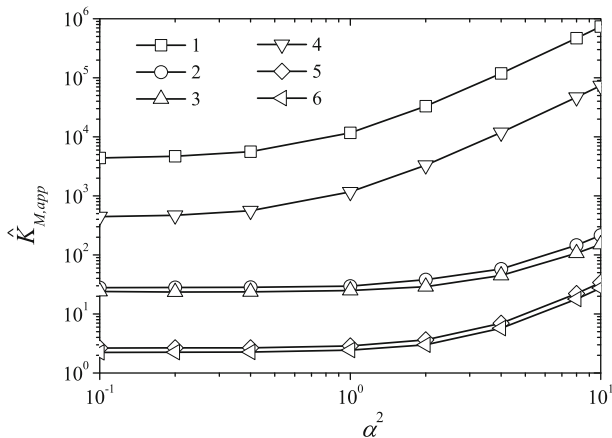


**Fig. 4** The apparent Michaelis constant  $\hat{K}_{M,app}$  versus the diffusion module  $\alpha^2$ ,  $Bi$ : 0.1 (1, 4), 10 (2, 5), 100 (3, 6),  $T_F$ : 1 (1–3), 10 s (4–6)

As one can see in Fig. 4 that  $\hat{K}_{M,app}$  is a monotonous increasing function of  $\alpha^2$ . When the enzyme kinetics predominates in the response ( $\alpha^2 < 1$ ) of a FIA biosensing system with a relatively large Biot number ( $Bi \geq 10$ ), the  $\hat{K}_{M,app}$  is approximately a constant function (curves 2, 3, 5 and 6). When the biosensor response is under diffusion control ( $\alpha^2 > 1$ ), the  $\hat{K}_{M,app}$  exponentially increases with an increase in the diffusion module  $\alpha^2$ . These features were particularly noticed in Figs. 2 and 3.

In real applications of biosensors, the diffusion module  $\alpha^2$  can be modified by changing the enzyme activity ( $V_{max}$ ) as well as the thickness  $d$  of the enzyme layer. The maximal enzymatic rate  $V_{max}$  is actually a product of two parameters: the catalytic constant  $k_2$  and the total concentration  $E_t$  of the enzyme [1, 3]. It is usually impossible to modify the  $k_2$  part. The maximal rate  $V_{max}$  might be modified by changing the enzyme concentration  $E_t$  in the enzyme layer.  $V_{max}$  is relative to the total enzyme used in a biosensor.

In the batch analysis ( $T_F \rightarrow \infty$ ), when the enzyme kinetics distinctly predominates in the biosensor response ( $\alpha^2 \ll 1$  and  $Bi \rightarrow \infty$ ), the apparent Michaelis constant  $K_{M,app}$  approaches the theoretical Michaelis constant  $K_M$ , i.e.  $K_{M,app} \approx K_M$ ,  $\hat{K}_{M,app} \approx 1$  [1, 3, 28, 31, 32]. As one can see in Figs. 2, 3 and 4 that  $\hat{K}_{M,app}$  is rather near to 1 also in the case of the FIA biosensing systems when  $\alpha^2 < 1$ ,  $T_F = 10$  and  $Bi = 100$ .

## 5 Conclusions

The mathematical model (3)–(9) of the flow injection analysis system based on an amperometric biosensor can be successfully used to investigate the kinetic peculiarities of the biosensor response. The corresponding dimensionless mathematical model (13)–(19) can be used as a framework for numerical investigation of the impact of model parameters on the biosensor action and to optimize the biosensor configuration.

By increasing the thickness  $\delta$  of the external diffusion layer or by decreasing the substrate diffusivity  $D_{S_2}$  in this layer (by decreasing the Biot number  $Bi$ ), the calibration curve of the biosensor can be prolonged by a few orders of magnitude. At relatively large values of the Biot number ( $Bi > 10$ ) the apparent Michaelis constant  $K_{M,app}$  is almost insensitive to changes in  $Bi$  (Fig. 2).

The apparent Michaelis constant  $K_{M,app}$  exponentially increases with a decrease in the injection time  $T_F$ . The calibration curve of the biosensor can be prolonged by a few orders of magnitude only by decreasing the injection time  $T_F$ . The impact of  $T_F$  is practically invariant to the Biot number  $Bi$  and the diffusion module  $\alpha^2$ . The exponential increase is specifically characteristic at low values of  $T_F$  ( $T_F < 3s$ ) (Fig. 3).

The  $K_{M,app}$  is a monotonous increasing function of the diffusion module  $\alpha^2$ . When the enzyme kinetics distinctly predominates in the response ( $\alpha^2 < 1$  and  $Bi \geq 10$ ), the  $K_{M,app}$  is approximately a constant function, while at  $\alpha^2 > 1$  the  $K_{M,app}$  exponentially increases with an increase in  $\alpha^2$  (Fig. 4).

**Acknowledgments** This work was partially supported by Lithuanian State Science and Studies Foundation, project No. PBT-04/2010.

## References

1. H. Gutfreund, *Kinetics for the Life Sciences* (Cambridge University Press, Cambridge, 1995)
2. A.P.F. Turner, I. Karube, G.S. Wilson, *Biosensors: Fundamentals and Applications* (Oxford University Press, Oxford, 1987)
3. F.W. Scheller, F. Schubert, *Biosensors* (Elsevier Science, Amsterdam, 1992)
4. U. Wollenberger, F. Lisdat, F.W. Scheller, *Frontiers in Biosensorics 2, Practical Applications* (Birkhauser, Basel, 1997)
5. B.E. Rapp, F.J. Gruhl, K. Länge, *Anal. Bioanal. Chem.* **398**, 2403 (2010)
6. S. Viswanathan, H. Radecka, J. Radecki, *Monatsh. Chem.* **140**, 891 (2009)
7. A.K. Wanekaya, W. Chen, A. Mulchandani, *J. Environ. Monit.* **10**, 703 (2008)
8. H.L. Schmidt, *J. Biotechnol.* **31**, 5 (1993)
9. L.D. Mello, L.T. Kubota, *Food Chem.* **77**, 237 (2002)
10. R. Nenkova, R. Atanasova, D. Ivanova, T. Godjevargova, *Biotechnol. Biotechnol. Eq.* **24**, 1986 (2010)
11. H. Lüdi, M.B. Garn, P. Bataillard, H.M. Widmer, *J. Biotechnol.* **14**, 71 (1990)
12. C. Tran-Minh, *J. Molec. Recogn.* **9**, 658 (1996)
13. B. Prieto-Simon, M. Campas, S. Andreeescu, J.L. Marty, *Sensors* **6**, 1161 (2006)
14. P. Cervini, E.T.G. Cavalheiro, *J. Braz. Chem. Soc.* **19**, 836 (2008)
15. M. Piano, S. Serban, R. Pittson, G.A. Drago, J.P. Hart, *Talanta* **82**, 34 (2010)
16. M.C.Q. Oliveira, M.R.V. Lanza, A.A. Tanaka, M.D.P.T. Sotomayor, *Anal. Methods.* **2**, 507 (2010)
17. C. Amatore, A. Oleinick, I. Svir, N. da Mota, L. Thouin, *Nonlinear Anal. Model. Contr.* **11**, 345 (2006)
18. L. Liu, *J. Math. Chem.* **47**, 1154 (2010)
19. M.E.G. Lyons, *Sensors* **6**, 1765 (2006)
20. L.D. Mell, T. Maloy, *Anal. Chem.* **47**, 299 (1975)
21. J. Kulys, *Anal. Lett.* **14**, 377 (1981)
22. P.N. Bartlett, R.G. Whitaker, *J. Electroanal. Chem.* **224**, 27 (1987)
23. T. Schulmeister, *Sel. Electrode Rev.* **12**, 203 (1990)
24. R. Baronas, F. Ivanauskas, J. Kulys, *Mathematical Modeling of Biosensors, Springer Series on Chemical Sensors and Biosensors, vol. 9* (Springer, Dordrecht, 2010)
25. S. Zhang, H. Zhao, R. John, *Electroanal* **13**, 1528 (2001)
26. R. Baronas, F. Ivanauskas, J. Kulys, *J. Math. Chem.* **32**, 225 (2002)
27. F. Ivanauskas, R. Baronas, *Int. J. Numer. Meth. Fluids* **56**, 1313 (2008)
28. F. Ivanauskas, I. Kaunietis, V. Laurinavicius, J. Razumiene, R. Simkus, *J. Math. Chem.* **43**, 1516 (2008)

29. R. Baronas, F. Ivanauskas, R. Maslovskis, M. Radavicius, P. Vaitkus, *Kybernetika* **47**, 21 (2007)
30. D. Britz, *Digital Simulation in Electrochemistry, Lecture Notes in Physics, vol. 666* (Springer, Berlin, 2005)
31. D. Olea, O. Viratelle, C. Faure, *Biosens. Bioelectron.* **23**, 788 (2008)
32. O. Stikoniene, F. Ivanauskas, V. Laurinavicius, *Talanta* **81**, 1245 (2010)
33. L.A. Segel, M. Slemrod, *SIAM Rev.* **31**, 446 (1989)
34. J.P. Kernevez, *Enzyme Mathematics, Studies in Mathematics and Its Applications* (Elsevier Science, Amsterdam, 1980)
35. M.E.G. Lyons, T. Bannon, G. Hinds, S. Rebouillat, *Analyst* **123**, 1947 (1998)
36. D. Britz, R. Baronas, E. Gaidamauskaite, F. Ivanauskas, *Nonlinear Anal. Model. Control* **14**, 419 (2009)
37. W.H. Press, S.A. Teukolsky, W.T. Vetterling, B.P. Flannery, *Numerical Recipes in C: The Art of Scientific Computing, 2nd edn* (Cambridge University Press, Cambridge, 1992)
38. D.A. Gough, J.K. Leypoldt, *Anal. Chem.* **51**, 439 (1979)